In-Situ Nucleation and Growth of γ-FeOOH Nanocrystallites in Polymeric Supramolecular Assemblies

Ashim K. Dutta, Gabriel Jarero,† Liqin Zhang, and Pieter Stroeve*

Center on Polymer Interfaces and Macromolecular Assemblies (CPIMA), Department of Chemical Engineering and Materials Science, University of California Davis, Davis, California 95616

Received August 12, 1999. Revised Manuscript Received November 1, 1999

This paper reports the nucleation and growth of lepidocrocite (γ-FeOOH) crystallites in supramolecular polymer multilayers. Organized, polymeric thin films were formed by the layer by layer deposition technique that consisted of adsorbing alternate layers of a polycation and a polyanion on a quartz substrate. Nucleation of nanoparticles was initiated by absorbing ferric nitrate in the thin film polymer matrix, followed by hydrolysis with ammonium hydroxide. Repeating the above process resulted in an increase in the density of the nanoparticles initially formed and further growth in the dimensions of the crystallites with the number of absorption and hydrolysis cycles. Analysis of the UV−visible absorption spectra of the films revealed the formation of lepidocrocites, which was confirmed by FTIR and selected area electron diffraction (SAED) studies. An important feature of this work is that lepidocrocite (γ-FeOOH) is formed instead of akaganéite (β-FeOOH), which is generated when ferrous chloride is used as the starting material and is converted to iron oxyhydroxide through oxidative hydrolysis as reported in our previous work (*Langmuir* **1999**, *15*, 2176). It therefore seems likely that the initial starting material plays a key role in determining the structural and morphological characteristics of the iron oxyhydroxides although their chemical compositions are the same.

Introduction

In recent years, there has been considerable interest in the nucleation of inorganic nanoparticles and the study of the growth in various matrices exhibiting constrained geometries such as zeolites, membranes, micelles, vesicles, cells, Langmuir−Blodgett (LB) films, and polymers.[1−3] While one standard approach involves the development of chemical methods for synthesizing inorganic solids of desired composition, structure, and morphology, an alternative simple and unique approach involves in-situ nucleation of nanoparticles in highly organized supramolecular assemblies[1−6] and their subsequent controlled growth into highly organized crystallites. The controlled growth and the formation of crystallites and even metallic particles of definite morphology and dimensions are possible today.[6] These studies have not only paved the way for a better understanding of the crystallization processes in orga-

* To whom all correspondence should be addressed. Phone: (530) 752-8778. Fax: (530) 752-1031. E-mail: pstroeve@ucdavis.edu.

† Present address: University of Texas−Pan American, College of Science and Engineering, Edinburg, TX 78539.

(1) (a) Mann, S., Webb, J., Willams, R. J. P., Eds. *Biomineralization, Chemical and Biochemical Perspectives*; VCH: Germany, 1989. (b) Wainwright, S. A.; Biggs, W. D.; Currey, J. D.; Gosline, J. M. *Mechanical Design in Organisms*; Princeton University Press: Princeton, NJ, 1976. (c) Weiner, S. *CRC Crit. Rev. Biochem*. **1986**, *20*, 325. (d) Sikes, C. S.; Wheeler, A. P. *Chemical Aspects of Regulation of Mineralization*; University of South Alabama Publication Service; Mobile, AL, 1988. (e) Lowenstam, H. A.; Weiner, S. *On Biomineralization*; Oxford University Press: New York, 1989.

(2) (a) Mann, S.; Archibald, D. D.; Didymus, J. M.; Douglas, T.; Heywood, B. R.; Meldrum, F. C.; Reeves, N. J. *Science* **1993**, *261*, 1286. (b) Heywood, B. R.; Mann, S. *Langmuir* **1992**, *8*, 1492. (c) Rajam, S.; Heywood, B. R.; Walker, J. B. A.; Mann, S.; Davey, R. J.; Birchall, J. D. *J. Chem. Soc., Faraday. Trans.* **1991**, *87*, 727. (d) Mann, S.; Heywood, B. R.; Rajam, S.; Birchall, J. D. *Proc. R. Soc. London, Ser. A* **1989**, *423*, 457.

(3) (a) Addadi, L.; Moradian, J.; Shay, E.; Maroudas, N. G.; Weiner, S. *Proc. Natl. Acad. Sci. U.S.A.* **1987**, *84*, 2732. (b) Addadi, L.; Weiner, S. *Proc. Natl. Acad. Sci. U.S.A.* **1985**, *82*, 4110. (c) Landau, E. M.; Levanon, M.; Leiserowitz, L.; Lahav, M.; Sagiv, J. *Nature* **1985**, *318*, 353. (d) Rieke, P. C. *Mater. Sci. Eng. C* **1995**, 181. (e) Rieke, P. C.; Marsh, B. D.; Wood, L. L.; Tarasevich, B. J.; Liu, J.; Song, L.; Fryxell, G. E. *Langmuir* **1995**, *11*, 318. (f) Stroeve, P.; Nagtegaal, M.; Tremel, W.; Knoll, W. *Polym. Preprints* **1997**, *38*, 965.

(4) (a) Furhop, J.-H.; Koning, J. *Membranes and Molecular Assemblies: The Synkinetic Approach*; The Royal Society of Chemistry, London, 1994. (b) Houslay, M. D.; Stanley, K. K. *Dynamics of Biological Membranes*, John-Wiley & Sons: N. Y. 1982. (c) Tien, H. T. *Bilayer Lipid Membranes. Theory and Practice*; Marcell Dekker: New York, 1974. (d) Fendler, J. H. *Membrane Mimetic Chemistry*; Wiley-Interscience: New York, 1982. (e) Kotov, N. A.; Meldrum, F. C.; Wu, C.; Fendler, J. H. *J. Phys. Chem*. **1994**, *98*, 2735. (f) Kotov, N. A.; Meldrum, F. C.; Wu, C.; Fendler, J. H. *J. Phys. Chem*. **1994**, *98*, 8827. (g) Yi, K. C.; Sanchez-Mendita, V.; Lopez Castanares, R.; Meldrum, F. C.; Fendler, J. H. *J. Phys. Chem*. **1995**, *99*, 9869.

(5) (a) Ulman, A. *An Introduction to Ultrathin Organic Films: from Langmuir−Blodgett to Self −Assembly*; Academic Press: Boston, 1991. (b) Roberts, G. *Langmuir−Blodgett Films*; Plenum Press: New York, 1990. (c) Gaines, G. L. *Insoluble Monolayers at Liquid−Gas Interfaces*; Interscience Publishing: New York, 1966.

(6) (a) Pileni, M. P., Eds. *Structure and Reactivity in Reverse Micelles*; Elsevier: Amsterdam, 1989. (b) Pileni, M. P.; Brochett, P.; Zemb, T.; Milhaud, J. *Surfactants in Solution*; Mittal, K. L., Bothorel, P., Eds.; Marcel-Dekker: New York, 1986. (c) Bawendi, M. G.; Steigerwald, M. L.; Brus, L. E. *Annu. Rev. Phys. Chem*. **1990**, *41*, 477. (d) Pileni, M. P. In *Handbook of Surface and Colloid Chemistry*; Birdi, K. S., Ed.; CRC Press: New York, 1997. (e) Fendler, J. H.; Fendler, E. J. *Catalysis in Micellar and Macromolecular Systems*; Academic Press: New York, 1975. (f) Fendler, J. H.; Meldrum, F. C. *Adv. Mater*. **1995**, *7*, 607.

10.1021/cm990522h CCC: $19.00
Published on Web 12/23/1999

nized biological systems but have also attracted the attention of the physicist, chemist, and materials scientist alike as the optical and electronic properties of these nanodimensional systems are different from their bulk properties that make them extremely important in designing the nanotechnology-based optical and electronic devices of the future.[7,8] Recent studies have established that, by fine-tuning the size and local environment of ordered supramolecular assemblies such as reverse micelles and vesicles, size dependent quantization/quantum confinement effects may be realized, resulting in significant changes in the optical and electronic properties of these systems, and the ability to fine-tune them for desired applications makes such systems extremely attractive.[7,8]

Oxides of iron, nickel, and cobalt exhibit interesting magnetic properties that find considerable technological applications in the area of recording devices, memory storage units, and color-imaging processors.[8] Extensive studies have revealed that at least 16 different oxides, hydroxides, and oxyhydroxides of iron are possible, and the final products depend on the pH, rate of oxidation, reaction conditions, and local microenvironment in which the reaction occurs.[9]

Interestingly, the crystal morphology, crystallinity, surface properties, and hence optical and electronic properties are largely dependent on the methodology employed for synthesis of these metal oxides.[9] It was therefore thought that inducing the formation of the oxides and/or hydroxides in a geometrically constrained environment such as that in an ordered supramolecular layer by layer polymer network[10] composed of alternate layers of polycations and polyanions could result in the formation of morphologically different crystallites of iron oxides having superior optical and magnetic properties compared to those of oxides prepared by other conventional means.

In this work, we have studied the nucleation and growth of lepidocrocite crystals in an organized supramolecular thin film polymeric network generated as a result of a layer by layer adsorption of polydiallyldimethylammonium chloride (PDDA) and polystyrenesulfonate sodium salt (PSS). This is in line with our previous studies on iron oxyhydroxide (FeOOH) nanocrystallites formed in polymer thin films[9] and self-assembled monolayers (SAMs).[11] Interest in the lepidocrocites stems from the fact that they are paramagnetic at room temperature, having a low Neel temperature of 77 K, and are easily converted into other industrially important magnetic oxides, namely maghemite and hematite, upon heating.[12]

Experimental Section

Poly(diallyldimethylammonium chloride) and polystyrenesulfonate (sodium salt), abbreviated as PDDA and PSS, respectively, were purchased from Polyscience Inc. (Warrington, Pa) and used as received. Ferric nitrate, ammonium hydroxide (29.6%), and hydrochloric acid (HCl) were products of Fisher scientific and used as received. PDDA (20 mM) solutions were prepared by dissolving it in deionized water obtained from a Millipore water purification system. PSS (20 mM) was however dissolved in a 0.1 M NaOH solution, and the pH was finally adjusted to 4.5 by dropwise addition of HCl (12 N).

Fluorescence grade optically flat quartz slides were used as the substrates for depositing polymeric multilayers. Prior to the deposition of the multilayers, the quartz slides were cleaned in Piranah solution (H_2O_2/H_2SO_4 3:7 v/v) maintained at 80 °C in a hot water bath and then washed thoroughly in deionized water. The Piranha solution treatment removes all traces of organic materials sticking to the quartz surface in addition to making the surface hydrophilic, as described in detail elsewhere.[9b] **Extreme caution must be exercised while using Piranha solution, as H_2O_2 forms an explosive mixture with H_2SO_4 and is extremely corrosive.**

Polymer thin films of alternate layers of PDDA and PSS on quartz slides were obtained by the layer by layer deposition technique that consisted of dip coating the slides alternately with PDDA and PSS solutions. Briefly, the previously cleaned substrates were kept dipped in the polyionic solutions for 15 min, thereby allowing sufficient time for the adsorption of the polyions onto the quartz surfaces. The slides were dried and then rinsed with pure deionized water and HCl before dipping them in the second polyion solution. A drying time of about 20 min was allowed between two consecutive dips. Absorption of metal ions within the polymer network was achieved by dipping the polymer film-coated slides in freshly prepared solutions of ferric nitrate (10 mM) taken in Schlenken tubes for 1 min. After the films were rinsed in deionized water and dried, they were dipped in an aqueous solution of ammonium hydroxide to undergo oxidative hydrolysis and form nanoparticles. In an effort to eliminate the effects of oxidation produced by dissolved gases, all solutions were thoroughly degassed by bubbling nitrogen through them for several hours prior to use and also during the hydrolysis process to provide a nitrogen-rich environment.

UV−visible absorption spectra of the thin polymer films deposited on quartz slides were recorded on a Cary-13 absorption spectrophotometer. FTIR measurements in the transmission mode were acquired on a Nicolet Protégé 460 spectrophotometer. For recording the FTIR spectrum, the polymer films were prepared on standard zinc selenide substrates.

(7) (a) Birge, R. R. *Molecular and Biomolecular Electronics*; American Chemical Society: Washington, DC, 1994. (b) *Materials and Measurements in Molecular Electronics*; Kajimura, K., Kuroda, S., Eds.; Springer Proceedings in Physics 81; Springer-Verlag: Tokyo, 1996. (c) Bosshard, C.; Sutter, K.; Pretre, P.; Hulliger, J.; Florsheimer, M.; Katz, P. *Organic Nonlinear Optical Materials*; Gordon and Breach: Basel, 1995. (d) Schieb, S.; Cava, M. P.; Baldwin, J. W.; Metzger, R. M. *Thin Solid Films* **1998**, *327−329*, 100. (e) *Molecular Electronics and Molecular Devices*; Seinicki, K., Ed.; CRC Press: New York, 1994.

(8) (a) Guenther, L. *Phys. World*. **1990**, *3*, 28. (b) Martin, C. R. *Acc. Chem. Res.* **1995**, *28*, 61. (c) Ziolo, R. F.; Giannelis, E. P.; Weinstein, B. A.; O'Horo, M. P.; Ganguly, B. N.; Mehrotra, V.; Russel, M. W.; Huffmann, D. R. *Science* **1992**, *257*, 219. (d) Ziolo, R. F.; Vassiliou, J. K.; Mehrotra, V.; Russel, M. W.; McMicheal, R. D.; Shull, R. D. *J. Appl. Phys.* **1993**, *73*, 5109. (e) McMicheal, R. P.; Schull, R. D.; Swartzendruber, L.; Bennet, L. H.; Watson, R. E. *J Magn. Magn. Mater.* **1990**, *85*, 219. (f) Winnik, F. M.; Morneau, A.; Ziolo, R. F.; Stroever, H. D. H.; Li, H. *Langmuir* **1995**, *11*, 3660.

(9) (a) Cornell, R. M.; Schwertmann, U. *The Iron Oxides, Structure, Properties, Reactions, Occurrence and Uses*; VCH: New York, 1996. (b) Dante, S.; Hou, Z.; Risbud, S.; Stroeve, P. *Langmuir* **1999**, *15*, 2176. (c) Tarasevich, B. J.; Rieke, P. C.; Liu, J. *Chem. Mater.* **1996**, *8*, 292. (d) Lewis, D. G.; Farmer, V. C. *Clay Miner.* **1986**, *21*, 93.

(10) (a) Decher, G. In *Comprehensive Supramolecular Chemistry*; Sauvage, J. P., Ed.; Pergamon Press: New York, 1996; Vol. 9, Chapter 14. (b) Decher, G.; Hong, J. D.; Schmitt, J. *Thin Solid Films* **1992**, *210/211*, 831. (c) Decher, G.; Lyov, Y.; Schmitt, J. *Thin Solid Films* **1994**, *244*, 772. (d) Ferreira, M.; Rubner, M. F. *Macromolecules* **1995**, *28*, 7107. (e) Fou, A. C.; Rubner, M. F. *Macromolecules* **1995**, *28*, 7115. (f) Korneev, D.; Lvov, Y. Decher, G.; Schmitt, J.; Yaradaikin, S. *Physica B* **1995**, *213−214*, 954.

(11) (a) Nagtegaal, M.; Stroeve, P.; Tremel, W. *Thin Solid Films* **1998**, *327−329*, 571. (b) Nagtegaal, M.; Stroeve, P.; Ensling, J.; Gutlich, P.; Schurrer, M.; Voit, H.; Flath, J.; Kashammer, J.; Knoll, W.; Tremel, W. *Chem. Eur. J.* **1999**, *5*, 1331.

(12) (a) Chopra, G. S.; Real. C.; Alcala, M. D.; Perez-Maqueda, L. A.; Subrt, J.; Craido, J. M. *Chem. Mater.* **1999**, *11*, 1128. (b) De Bakker, P. M. A.; De Grave, E. D.; Vandenberghe, R. E.; Bowen, L. H.; Pollard, R. J.; Persoons, R. M. *Phys. Chem. Miner.* **1991**, *18*, 331. (c) Ishikawa, T.; Inouye, K. *Bull. Chem. Soc. Jpn.* **1972**, *45*, 2530. (d) Naona, H.; Nakai, K. *J. Colloid Interface Sci.* **1989**, *128*, 146. (e) Gehring, A. U.; Karthein, R.; Reller, A. *Naturwissenschaften* **1990**, *77*, 177.

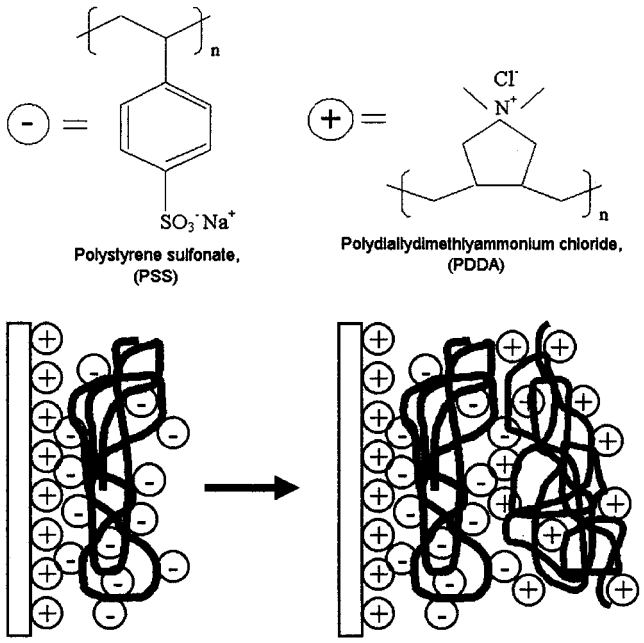

Figure 1. Schematic diagram of the formation of the layer by layer structure of PDDA and PSS on quartz substrates. Inset shows the molecular structures of PDDA and PSS.

Transmission electron microscopy (TEM) of the polymer films deposited on conventional electron microscope copper grids (300 mesh) coated with Formvar was used. A Hitachi H-600 transmission electron microscope was used for imaging the iron oxyhydroxide particles formed in the multilayered films and for structural analysis using selected area electron diffraction (SAED) analysis. Instead of the 10M concentration of ferric nitrate used for UV−vis absorption measurements, we have used a much lower concentration of ferric nitrate (2 mM) to obtain better quality images. For SAED measurements a gold layer (50 nm) was deposited on the grids such that the lattice parameters for gold may be utilized for instrumental calibration and quantitative interpretation of the diffraction patterns and hence identify the nature of the species formed by comparison with standard samples.

Results and Discussion

The layer by layer deposition technique used to build multilayers has emerged as a simple, yet elegant and reliable, means of building ordered multilayers of polymers on substrates. Briefly, the hydrophilic end groups attached to the polymer are adsorbed on the hydrophilic substrate through hydrophilic interactions and the polymer-coated surface gets charged. Using a counter polyion, layer by layer assemblies can be built up as shown in the schematic of Figure 1. Extensive works by Decher et al.[10a−c] have established that as many as 100 layer pairs may be reproducibly and reliably built on supports, thereby constituting a robust and highly stable multilayered system.

Figure 2 shows the normalized absorption spectra of a pristine polymer film composed of alternate layer pairs of PDDA and PSS. The UV−visible absorption spectrum in the 200−500 nm region shows a band at 225 nm that arises from the aromatic group present in the PSS molecule. It was confirmed from the absorption spectrum of a cast film of PDDA on quartz that this band does not arise from PDDA. Monitoring this band at 225 nm, it was confirmed that the absorbance increased linearly with the number of layer pairs transferred onto the quartz substrates (figure not shown). A maximum

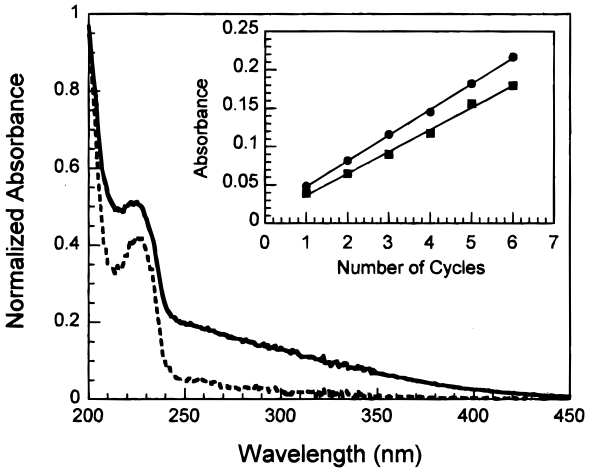

Figure 2. Absorption spectra of (a) a 3.5 layer pairs film of PDDA and PSS deposited on a quartz slide by the layer by layer technique (dotted line) and (b) the same film treated consecutively with ferric nitrate and ammonium hydroxide (6 cycles) (solid line). The concentration of ferric nitrate was 10 mM. The inset shows the plot of absorbance corresponding to the absorption bands at 290 nm (filled circles) and at 320 nm (filled squares), respectively, versus the number of absorption and hydrolysis cycles. Each complete cycle consists of absorbing ferric nitrate in the polymeric films followed by a water rinse and hydrolysis using ammonium hydroxide.

of six layer pairs were studied in this work, and the linear increase in absorbance with the number of layer pairs transferred onto the quartz substrates confirms that indeed the layers are reproducibly transferred onto the substrates. In this context, it is worthwhile to point out that PDDA was used instead of PAA (polyallylamine), as PAA/PSS films were found to be unstable and tended to be washed off after repeated dipping cycles. On the other hand, PDDA/PSS films are found to be robust and stable.

Figure 2 also shows the absorption spectrum of the polymer film after undergoing six consecutive cycles of ferric nitrate absorption and hydrolysis with ammonium hydroxide. The spectral profile is clearly different from that of the pristine polymer film, confirming the presence of iron hydroxides and/or oxides in the film. The plots of absorbance versus the number of absorption−hydrolysis treatment cycles to which the films have been exposed are shown in the inset of Figure 2. The straight-line profile of the curves confirms that the process of absorption of ferric nitrate in the polymeric films and its subsequent conversion to the oxyhydroxide is indeed a reproducible process. Although the reaction process is not clear, the first step probably involves the binding of the iron species[9b] with the sulfonate groups in the PSS, which is then followed by the oxidative hydrolysis of these species.

Figure 3a shows the absorption spectrum of a layer by layer film of PDDA and PSS doped with 20 mM ferric nitrate solution and subjected to 20 hydrolysis cycles. Careful inspection of the absorption spectrum reveals a strong buildup in absorbance in the 250−500 nm region, owing to the formation of ferric oxyhydroxide. The broad band profile with a knee at about 350 nm confirms the presence of ferric oxyhydroxide and is in excellent agreement with published data.[9] In this context, it must be pointed out that iron oxides and oxyhydroxide may have different chemical compositions depending upon the method of preparation and such

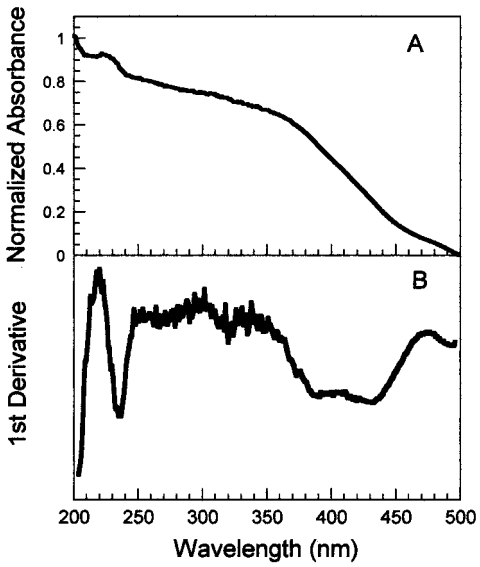

Figure 3. (a) Absorption spectra of (a) iron oxyhydroxide formed in the polymeric network generated by the layer deposition of PDDA and PSS on a quartz slide. (b) First derivative of the absorption spectrum shown in part a. The concentration of ferric nitrate was 20 mM.

parameters as pH, presence of ions, local environment, temperature, and aging times.[9a] Moreover, their morphological structures also depend on all these factors, which makes exact identification of the species difficult, as all these above factors cause considerable changes in the electronic spectra of these materials.[9,11] The structures region (250−350 nm) probably consists of overlapping bands corresponding to different electronic transitions that may be resolved by derivative spectroscopy. Extensive works by several authors[9a,c] have demonstrated that indeed derivative spectroscopy does provide much insight in identifying the various components present in an assortment of different species, as in mineralogical samples. The first derivative of the absorption spectrum shown in Figure 3b reveals peaks at 210, 240, 304, 359, 434, and 485 nm. While the band at 210 nm correspond to the charge-transfer (CT) transition, the bands at 240 and 304 nm corresponds to the $^6T_{1u}-2t_{1u}$ and $^6A_1-^4$ T_1 transitions.[9a] The other three bands at 359, 434, and 485 correspond to the well-known transitions $^6A_1-^4$ E, $^6A_1-^4A_1$, and $2(^6A_1)-2(^4T_1)$, and these are in excellent agreement with those reported in the literature[9a] for standard lepidocrocite (γ-FeOOH) samples. These results confirm that indeed lepidocrocite (γ-FeOOH) is formed in the layered polymeric films.

Figure 4 represents the transmission FTIR spectra of a thin film of PDDA and PSS subjected to alternate absorption with ferric nitrate solution and subsequent hydrolysis with ammonium hydroxide. The spectrum shows a band at 3181 cm^{-1} corresponding to the OH stretching mode, and the bands at 1171 and 1012 cm^{-1} corresponds to the OH in-plane bending mode of the B_{2u} and B_{3u} transition moments. The peak at 762 cm^{-1} very likely corresponds to the out of plane bending moment of the B_{1u} transition. These results are in agreement with the vibronic structure for iron oxyhydroxide reported by Lewis and Farmer.[9d] The observed differences in the spectral profile and shift of the band maximum position probably arise from the highly ordered structure of the iron oxyhydroxide aggregates produced in

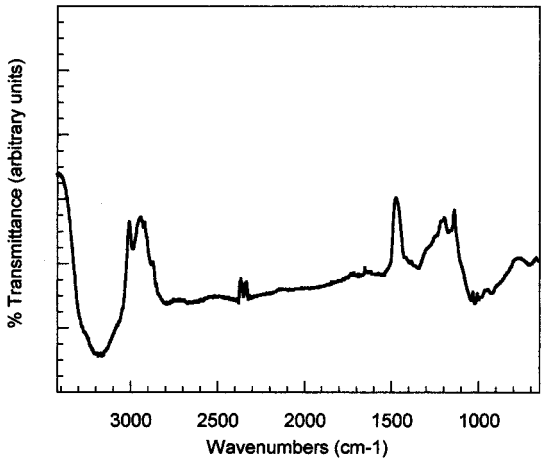

Figure 4. FTIR spectrum of lepidocrocite crystallites in a 3.5 layer pairs film of PDDA and PSS. The film was prepared on ZnSe substrates and subjected to six cycles of absorption and hydrolysis. The ferric nitrate concentration was 30 mM.

the supramolecular polymer network.[5] Cast films of lepidocrocite produced by dip coating slides with iron oxyhydroxide show bands (spectra not shown) that correspond with those reported by Lewis et al.,[9d] confirming that the differences in the spectral profile originate from the high degree of crystallinity of lepidocrocite crystallites embedded in the polymer matrix.

Transmission electron microscopy (TEM) has emerged as a versatile technique used routinely to explore microscopic structures in detail down to the nanometer length scale. Panels a−d of Figure 5 show the TEM images of a 3.5 layer pairs of PDDA and PSS exposed to alternate cycles consisting of ferric nitrate absorption and its subsequent hydrolysis with ammonium hydroxide. Panel A represents the image corresponding to the initial stages of iron oxyhydroxide formation. The ferric nitrate concentration was maintained at 1 mM, and the film was exposed to only two cycles of absorption and hydrolysis. This micrograph (panel 5A) reveals dark patches corresponding to large agglomerates of iron oxyhydroxide that probably exist as nanoparticles. Increasing the magnification from 25K× to 100K× did not improve the resolution of the micrographs. It is possible that the sizes of the nanoparticles exceed the resolution of the electron microscope used in this work. Figure 5B demonstrates the effect of increasing the ferric nitrate concentration from 1 mM (Figure 5A) to 2 mM. In addition to the formation of a large number of densely packed crystals, a close look at the image reveals small isolated crystals in the background. These small clusters correspond to the crystallites of iron oxyhydroxide formed in the polymeric network, indicating systematic and organized growth of the nanoparticles into crystallites. Increasing the number of absorption−hydrolysis cycles also results in an increase in the size of these nanocrystallites, as demonstrated in Figure 5C. It is interesting to note that, in addition to the large well-defined crystallites formed, the understructure shows the formation of smaller crystallites at different stages of their growth process. Increasing the concentration further results in the formation of larger crystals. Careful examination of the crystallites shows that the ratio of the length to the width increases. In this context, it is worthwhile to point out that initially nanoparticles are generated that act as the nucleation center for the formation of crystallites. It may be further

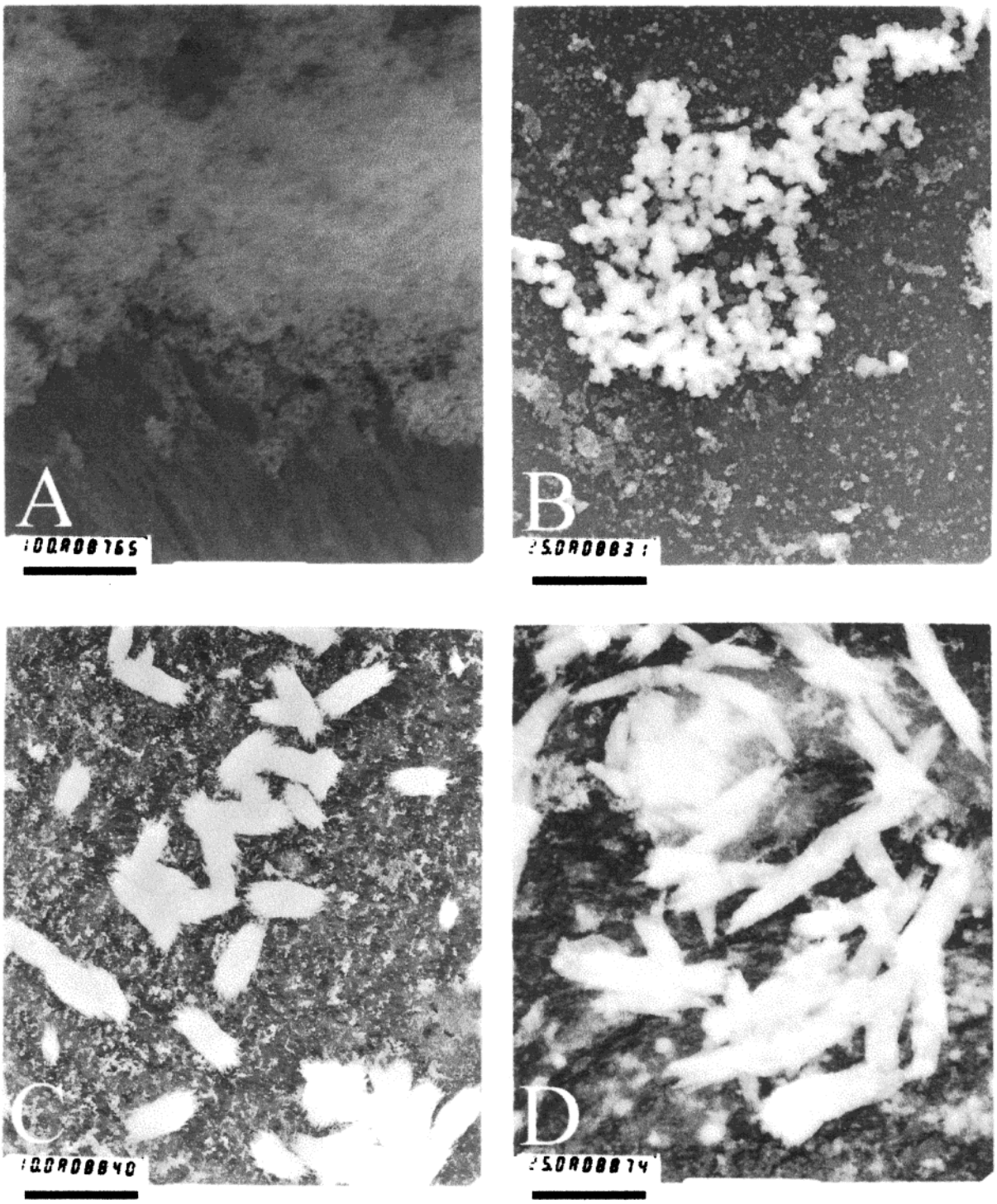

Figure 5. TEM micrographs of a 3.5 layer pairs film of PDDA and PSS at different stages of the crystallization process: (a) 1 mM ferric nitrate, two absorption−hydrolysis cycles, $M = 100\text{K}\times$, bar size 1 cm = 100 nm; (b) 2 mM ferric nitrate, two absorption−hydrolysis cycles, $M = 25\text{K}\times$, bar size 1 cm = 400 nm; (c) 2 mM ferric nitrate, eight absorption−hydrolysis cycles, $M = 10\text{K}\times$, bar size 1 cm = 1000 nm; (d) 4 mM ferric nitrate, four absorption−hydrolysis cycles, $M = 25\text{K}\times$, bar size 1 cm = 400 nm.

pointed out that although the formation of crystallites with a high degree of crystallinity indicates extensive local microscopic ordering, there seems to be little correlation between the alignment of the different crystallites in the polymeric network. One plausible explanation seems to be that nucleation of nanoparticles is a statistical phenomena that probably occurs randomly within the cavities; however, growth of the nanoparticles formed proceeds exponentially in time, resulting in the formation of microcrystallites. The growth and the shape of the crystallites may be controlled by the structure of the "nanoreactors" or voids in which nucleation and growth of the crystallites occur. Physical restrictions offered by the walls of the polymer cavities prevent growth of the crystallites in certain specific directions depending upon the nature of the cavities. In a polymeric network, the voids are usually interconnecting, and long channel-like cavities are formed that allow the crystallites to grow preferentially along the length of the channel, which probably accounts for an increase in the axial ratio of the crystallites, as observed from the TEM micrographs (Figure 5C and D).

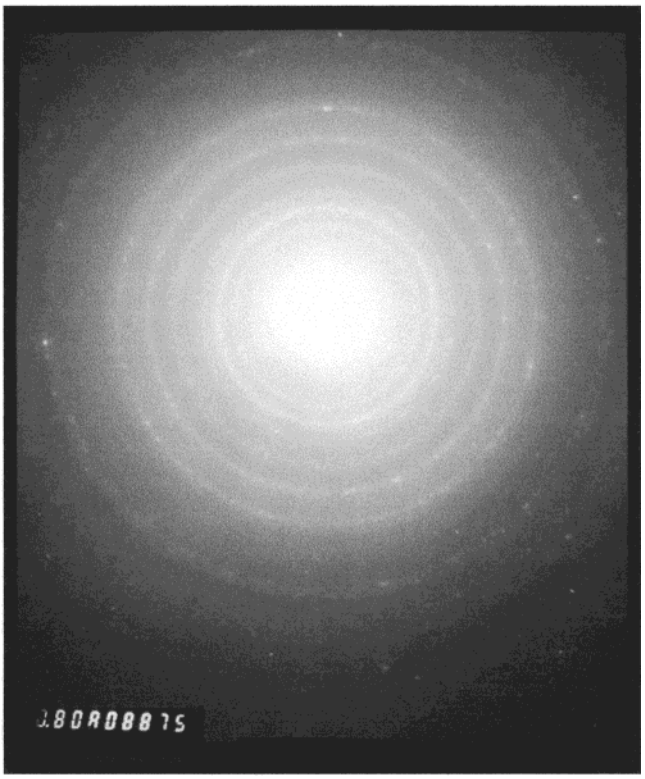

Figure 6. Selected area electron diffraction (SAED) pattern of ferric oxyhydroxide nanocrystallites formed in a 3.5 layer pairs PDDA−PSS films exposed to 4 mM ferric nitrate and subjected to four absorption−hydrolysis cycles.

Table 1

hkl	d_{calc}	d_{theo}	D_{calc}	D_{theo}	expt error (%)
2,2,0	0.1874	0.1853	31.59	31.94	1.09
0,8,0	0.1563	0.1568	37.88	37.75	0.34
1,9,0	0.1329	0.1311	44.53	45.15	1.37
2,4,2	0.1133	0.1124	52.28	52.66	0.72
0,14,0	0.0904	0.0896	65.42	64.34	1.67

Eventually, as the number of reaction cycles is increased and the particles grow, there is a point at which the particles will start to deform the film because of their thicknesses.

Figure 6 shows the selected area electron diffraction (SAED) pattern of the ferric oxyhydroxide crystallites as shown in Figure 5D. The presence of the concentric rings with bright spots confirms a high degree of molecular ordering in these crystallites. Utilizing the mathematical relation, $\lambda L = d(D/2)$, where λ is the De-Broglie wavelength for the accelerated electron, L is the length of the camera, d is the lattice spacing, and D is the diameter of the diffraction ring, we have evaluated the lattice parameter d. The De-Broglie wavelength of the electron accelerated at 100 kV is 3.7×10^{-3} nm, and the camera length used in this work was 0.8 m. Comparing the d values obtained experimentally with that predicted theoretically by the electron microscopy simulation software program developed by CIOLS−Laussanne (Table 1), it is evident that indeed the crystallites do represent lepidocrocites. The theoretical calculations using the software program assume an ideal lepidocrocite crystal to be orthorhombic, having $a = 0.3880$ nm, $b = 1.2540$ nm, and $c = 0.3070$ nm, and the space group corresponds to $D^{17}{}_{2h}$ *Cmcm*. Lepidocrocite has a typical layered structure in contrast to the tunnel-like structures of other iron polymorphs, namely géotheite (α-FeOOH) and akaganéite (β-FeOOH).[9] In this connection, it is worthwhile to point out that attempts were made to match the data obtained by us with the standard data of akaganéite and géotheite. Careful comparison showed a complete mismatch; in addition, several specific lines characteristic of the two different species were found to be missing, providing compelling evidence that our data do not resemble those of either of the two.[13] On the contrary, an excellent match was obtained with that of lepidocrocite, suggesting its formation in the polymer matrix.

It is worthwhile to note here that although lepidocrocite crystallites are formed when ferric nitrate undergoes oxidative hydrolysis in the PDDA−PSS supramolecular assemblies, akaganéite crystallites are formed when ferrous chloride is used, as demonstrated in our previous work.[9b] These findings clearly demonstrate that the starting material and, in particular, the anion play a crucial role in determining the morphological structure of the iron oxyhydroxide finally formed in the polymer matrix. The akaganéite structure contains tunnels, which are stabilized by chloride ions.[9a] In fact akaganéite is found naturally only in chloride-rich environments such as hot brine springs and acid mine waters.[9a]

Conclusions

We have studied the formation of iron oxyhydroxide nanoparticles in organized supramolecular polymer thin films. These films were successfully prepared by absorbing a polycation and a polyanion alternately on quartz substrates, giving rise to a robust and porous supramolecular matrix. Nanoparticles of iron oxyhydroxide are formed by absorbing ferric nitrate in these films followed by hydrolysis with ammonium hydroxide. Detailed spectral analysis of the films using UV−visible absorption spectroscopy reveals bands that correspond with that of lepidocrocite, confirming its presence in these films. FTIR and SAED studies also substantiate these findings. The morphology of the films in which the growth of the iron oxyhydroxide particles has been induced was studied as a function of ferric nitrate concentration and the number of absorption and hydrolysis cycles. It is evident that, with increasing ferric nitrate concentration and the number of absorption and hydrolysis cycles, the size of the crystallites increases, in accordance with the nucleation and growth theory. A comparison of these results with our previous studies, where akaganéite was generated as a result of oxidative hydrolysis of ferrous chloride,[9b] clearly demonstrates that the morphology of the end products is dependent on the route of the reaction process.

Acknowledgment. This work was partially supported by CPIMA (NSF Grant DMR-9808677). G.J. was a CIPMA SURE undergraduate for summer 1999.

CM990522H

(13) For crystal structure of iron oxides see Internet site http://cimewww.epfl.ch/CIOLS.